

Au Hierarchical Micro/Nanotower Arrays and Their Improved SERS Effect by Ag Nanoparticle Decoration

Chuhong Zhu,[†] Guowen Meng,^{*,†} Qing Huang,^{*,‡} Zhulin Huang,[†] and Zhaoqin Chu[†]

[†]Key Laboratory of Materials Physics, Anhui Key Laboratory of Nanomaterials and Nanostructures, Institute of Solid State Physics and [‡]Key Laboratory of Ion Beam Bioengineering, Hefei Institutes of Physical Science, Chinese Academy of Sciences, Hefei, 230031, China

Received September 27, 2010; Revised Manuscript Received January 5, 2011

ABSTRACT: Arrays of Au hierarchical micro/nanotowers have been achieved on Au-coated silicon planar substrate, via electrochemical deposition in a mixed aqueous solution of PVP and HAuCl₄ under appropriate electrodeposition conditions. The Au hierarchical micro/nanotower arrays have exhibited distinct surface-enhanced Raman scattering (SERS) effect due to the enhanced local electromagnetic field in the vicinity of the sharp nanotips of the towers and the gaps between the neighboring nanotowers. More importantly, the SERS effect has been further improved significantly via decorating Ag nanoparticles on the surfaces of the Au hierarchical micro/nanotowers due to the Ag nanoparticle hot spots themselves and the hot spots formed at the interfaces between the Ag nanoparticles and the Au micro/nanotowers. These Ag-nanoparticle-decorated Au hierarchical micro/nanotower arrays have shown potential applications as sensitive and robust SERS substrates in monitoring environmental pollutants, such as 3,3',4,4'-tetrachlorobiphenyl (PCB-77).

Introduction

Surface-enhanced Raman scattering (SERS) has been intensely studied for many years as a great potential tool for ultratrace detection.¹ Noble metal (especially Au and Ag) nanocrystals with different morphologies have been reported as SERS substrates, such as Au nano-octahedra,² nanoicosahedra,³ nanoflowers⁴ and sponges,⁵ and Ag nanocrescent,⁶ nanowires,⁷ nanorods,⁸ nanoplates,^{9,10} nanorings,¹¹ rough nanoparticles,¹² and dendrites.¹³ Among numerous morphologies of Au/Ag nanocrystals, arrays of nanotips are of special interest due to their extremely concentrated electromagnetic field at the tip apex, resulting in a great enhancement of the SERS signals from molecules located in the vicinity of the nanotips.¹⁴ Although a self-assembly based templating method could be used to fabricate Au nanotower arrays with sharp nanotips as SERS substrates,¹⁴ this method involves many complex steps. Therefore a simple low-cost direct growth of large-scale Au hierarchical micro/nanotower arrays on a planar substrate still remains a big challenge.

For SERS realization, hierarchical micro/nanostructures have stimulated much attention since such architectures combine the advantages of both micrometer- (stable, antiagglomeration and being easy to observe under optical microscopy) and nanometer-scaled (with much improved SERS effect) building blocks, and show unique properties much different from those of the monomorphological structures.^{12,15,16} On the other hand, the SERS effect of Au nanotip arrays could be further improved by decorating Ag nanoparticles due to both the Ag hot spots and the hot spots formed at the interface between Ag nanoparticles and the Au nanotips.^{17,18} Hence, decorating Ag nanoparticles on the surface of the Au micro- or nanostructure arrays may improve their SERS effect.

In this work, we present a low-cost electrochemical deposition of Au hierarchical micro/nanotower arrays growing

tightly on Au-coated Si planar substrate. The Au hierarchical micro/nanotower arrays showed distinct SERS effect due to their enhanced local electromagnetic field in the vicinity of the sharp tower tips and the gaps between the neighboring nanotowers. Furthermore, by decorating Ag nanoparticles on the surface of the Au hierarchical micro/nanotowers via a subsequent electrodeposition, hierarchical and hybrid arrays of Ag-nanoparticle-decorated Au micro/nanotowers have been achieved, and showed much stronger SERS effect.

Experimental Section

For the synthesis of Au hierarchical micro/nanotower arrays, 0.05 g of HAuCl₄·4H₂O and 1 g of poly(vinyl pyrrolidone) (PVP, MW = 30 000) were added to 50 mL of deionized (DI) water, and magnetically stirred until complete dissolution. Such an aqueous solution was used as the electrolyte in the electrodeposition of Au hierarchical micro/nanotower arrays. A 30–40 nm thick gold layer was sputtered onto the prepolished planar silicon wafers (2 cm × 0.5 cm). A graphite flake was used as anode and the Au-coated silicon wafer as cathode. The electrodeposition was carried out under a current density of 90 $\mu\text{A}/\text{cm}^2$ for 13 h at 40 °C. The Au-coated Si cathode (substrate) with products was then taken out, cleaned with DI water several times and dried in the air (step 1 in Figure 1). For further decorating Ag nanoparticles on the Au hierarchical micro/nanotower arrays, 0.1 g of AgNO₃ and 1 g of citric acid were added to 50 mL of DI water followed by stirring until complete dissolution. Using such an aqueous solution as the electrolyte, Ag nanoparticles were decorated onto the surface of the Au hierarchical micro/nanotowers grown on the Au-coated Si cathode via electrodeposition under a constant current density of 150 $\mu\text{A}/\text{cm}^2$ for 15 min at room temperature. The final products were then taken out, cleaned with DI water several times and dried in high-purity Ar (step 2 in Figure 1). Before SERS measurements, the Ag-nanoparticle-decorated hierarchical micro/nanotowers were cleaned by plasma to eliminate the citric acid on their surfaces. For checking their SERS activity, the Ag-nanoparticle-decorated hierarchical micro/nanotowers were placed in 2 mL of a R6G aqueous solution for 4 h. Afterward the Ag-nanoparticle-decorated hierarchical micro/nanotowers were taken out, rinsed with DI water, and allowed to dry in high-purity Ar. For the detection of PCB-77, the Ag-nanoparticle-decorated

*To whom correspondence should be addressed. E-mail: gwmeng@issp.ac.cn; huangq@ipp.ac.cn.

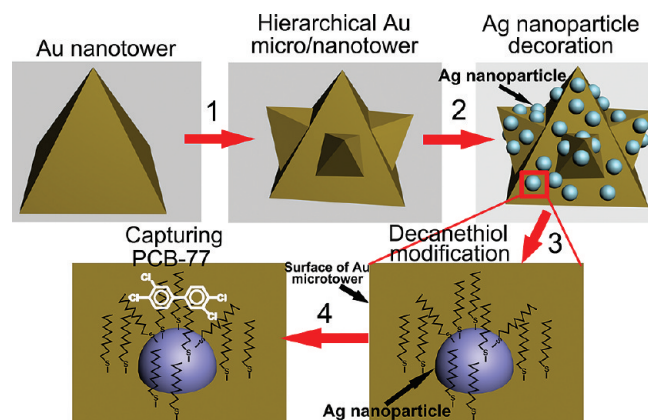


Figure 1. Schematic diagram for the fabrication of Au micro/nanotowers, subsequent surface decoration of Ag nanoparticles for improving their SERS effect, and then surface modification of decanethiol for effectively capturing target analyte PCB-77 molecules.

hierarchical micro/nanotowers were placed in 1 mL of a 1 mM ethanolic 1-decanethiol (which helps to capture PCB-77 molecules efficiently) solution for 16 h. Afterward the Ag-nanoparticle-decorated hierarchical micro/nanotowers were taken out, rinsed with ethanol, and allowed to dry in high-purity Ar (step 3 in Figure 1). Then the decanethiol-modified Ag-nanoparticle-decorated hierarchical micro/nanotowers were placed in 2 mL of a PCB-77 *n*-hexane solution for 4 h. Afterward the Ag-nanoparticle-decorated hierarchical micro/nanotowers were taken out, rinsed with ethanol, and allowed to dry in high-purity Ar (step 4 in Figure 1).

The resultant products were characterized by using X-ray diffraction (XRD) (Philips X'pert-PRO), scanning electronic microscope (SEM, sirion 200), transmission electron microscope (TEM, JEOL 2010) and ultraviolet–visible–near-infrared spectrophotometer (Hitachi, U-4100). SERS measurement was conducted on a confocal microprobe Raman system (LABRAM-HR, France), and the excitation wavelength was 514.5 nm from an air-cooled argon ion laser. The laser light was vertically projected onto the samples with a resultant beam intensity of $\sim 10^5 \text{ W cm}^{-2}$.

Results and Discussion

SEM observation (Figure 2a) on the Au-coated Si substrate reveals that, after electrodeposition of Au, the resultant products are arrays of three-dimensionally hierarchical Au micro/nanotowers with diameters of 0.3–0.7 μm . Detailed observation further reveals that some larger hierarchical micro/nanotowers comprise dozens of branches radiating from the stems (Figure 2b). XRD spectrum taken from the as-electrodeposited hierarchical micro/nanotowers detached from the Au-coated Si wafer (Figure 2c) reveals that all the diffraction peaks can be indexed to the face-centered-cubic (fcc) Au. The strong and sharp diffraction peaks imply that the as-electrodeposited hierarchical micro/nanotowers are well crystallized. The peak intensity ratio of $\{111\}$ to $\{200\}$ in the XRD spectrum is about 5, being higher than that of the bulk Au (about 2), indicating that the surfaces of the as-electrodeposited Au hierarchical micro/nanotowers have a tendency to be terminated by the lowest energy $\{111\}$ planes. TEM observation (Figure 2d) on a typical hierarchical micro/nanotower reveals that the primary stem tower is about 3 μm , with several branches. There are four asymmetrical rows of Au secondary branches growing on the four surfaces of the primary stems. TEM observation (Figure 2d), together with SEM observations (Figure 2a,b), reveals that the lengths of the stems are several micrometers, and the branches are about

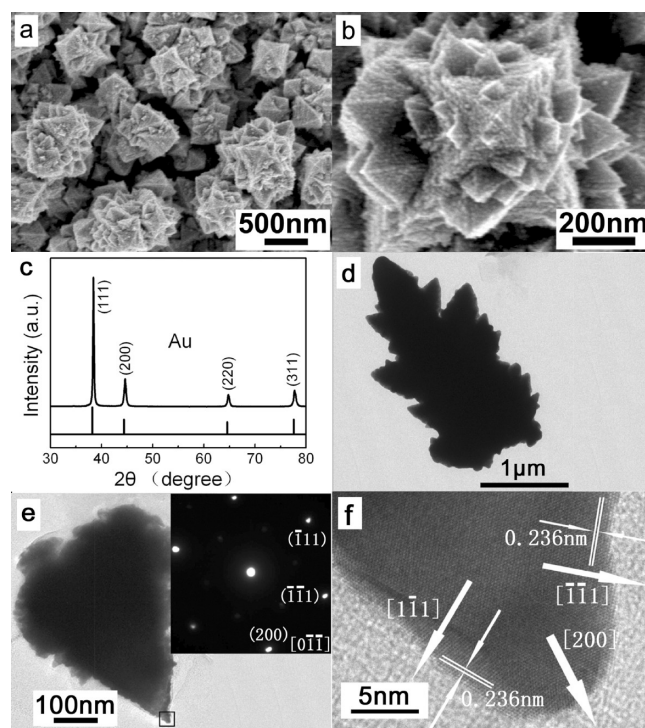


Figure 2. The Au hierarchical micro/nanotower arrays. SEM images of the as-electrodeposited Au samples at (a) low and (b) high magnifications. (c) XRD spectrum taken on the as-electrodeposited Au hierarchical micro/nanotower arrays. The lower spectrum is the standard diffraction of Au powders. (d) TEM image of a typical Au hierarchical micro/nanotower. (e) TEM and (f) HRTEM images of a representative Au tower. The inset in (e) is SAED pattern taken from the rectangle region marked in (e).

0.05–0.5 μm long. Figures 2e and 2f are TEM and high-resolution TEM images of a representative microtower with the corresponding selected area electron diffraction (SAED) pattern taken from its tip (inset in Figure 2e), which can be indexed to the $\langle 011 \rangle$ zone axis of Au. The high-resolution TEM image (Figure 2f) displays clear fringes with a spacing of $\sim 0.236 \text{ nm}$. From Figure 2e and 2f we can infer that the electron beam was parallel to the two side surfaces of the microtower. Therefore the clear fringes in Figure 2f imply that the Au microtower tip is a single crystal growing along the $[200]$ direction and enclosed by the $\{111\}$ planes as the side surfaces (marked in Figure 2f). Hence, the towers have a tendency to be terminated by the lowest energy $\{111\}$ planes being in agreement with the fact that the towers exhibit four symmetrical surfaces. Additionally, the SAED pattern (Figure S1b in the Supporting Information) taken from the edge of a micro/nanotower (shown in Figure S1a in the Supporting Information) indicates that the edge of the micro/nanotowers is polycrystalline, further confirming that the Au micro/nanotower is an assembly system.

A systematic experimental investigation (Supporting Information Part I) reveals that the electrodeposition current density, the concentrations of PVP and Au^{3+} in the electrolyte, and the electrolyte temperature remarkably affect the morphology of the resultant Au products. Only under the appropriate electrodeposition conditions, such as at the current density of 75–100 $\mu\text{A/cm}^2$, the PVP concentration of 15–30 g/L, the $\text{HAuCl}_4 \cdot 4\text{H}_2\text{O}$ concentration of 0.5–1.2 g/L and the electrolyte temperature of 35–50 $^\circ\text{C}$, can the Au hierarchical micro/nanotowers be achieved (Figures S2–4 in

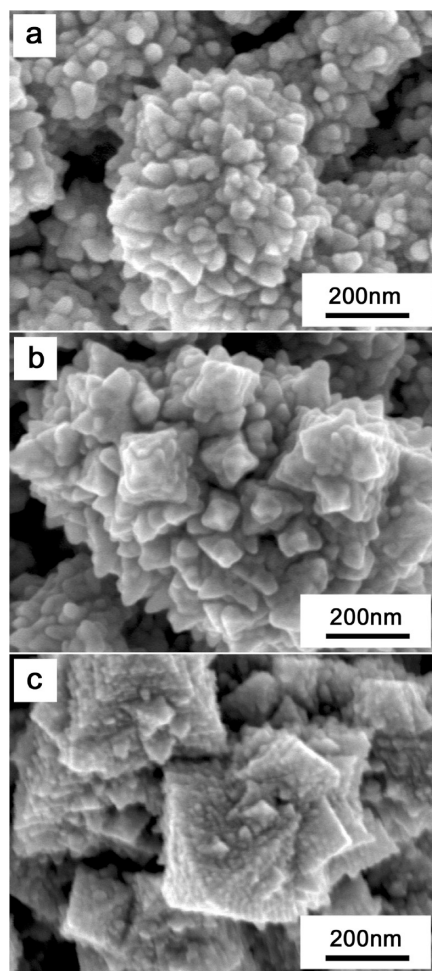


Figure 3. SEM images of the as-electrodeposited Au samples achieved at electrodeposition current density of $90 \mu\text{A}/\text{cm}^2$, with $\text{HAuCl}_4 \cdot 4\text{H}_2\text{O}$ concentration of 1 g/L and PVP concentration of 20 g/L for different electrodeposition durations of (a) 3 h, (b) 7 h, and (c) 11 h, respectively.

the Supporting Information). On the basis of these experiments, it can be concluded that quasi-equilibrium growth condition (low current density) and PVP preferential adsorption are crucial for the formation of the Au hierarchical micro/nanotowers. Higher current density promotes the nucleation and leads to the formation of the packed spherical particles (Figure S2d in the Supporting Information). PVP preferential adsorption is affected by the electrodeposition current density, the PVP concentration, and the Au^{3+} concentration. Lower PVP concentration,²⁸ lower current density and higher Au^{3+} concentration are all disadvantageous to the PVP preferential adsorption onto {111} facets of a Au crystal nucleus, and will lead to the formation of Au crystals with irregular morphologies (Figures S3a, S3b, S2a–c, S4b and S4c in the Supporting Information).

In order to reveal the formation process of the Au hierarchical micro/nanotowers in more detail, experiments were conducted for various durations of 3, 7, and 11 h, given the other conditions the same (with the electrodeposition current density of $90 \mu\text{A}/\text{cm}^2$, the PVP concentration of 20 g/L, the $\text{HAuCl}_4 \cdot 4\text{H}_2\text{O}$ concentration of 1 g/L and the electrolyte temperature of 40°C). Representative SEM images of the resultant products are shown in Figure 3. First, Au nanostructures with tips were formed after electrodeposition for 3 h

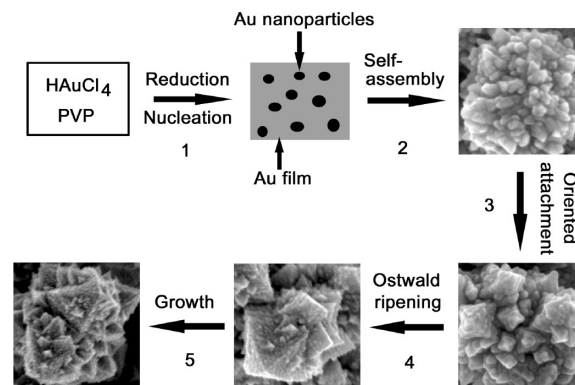


Figure 4. Schematic showing the formation process of the Au hierarchical micro/nanotowers.

(Figure 3a), then underdeveloped rough hierarchical micro/nanotowers were formed after electrodeposition for 7 h (Figure 3b), and well-assembled hierarchical micro/nanotowers with relatively smooth surfaces were formed after electrodeposition for 11 h (Figure 3c). When the electrodeposition was further prolonged to 13 h, well-crystallized Au hierarchical micro/nanotowers were finally achieved (Figure 2a,b).

A schematic illustration of the Au hierarchical micro/nanotower formation is presented in Figure 4. PVP is used to adjust the growth velocity of Au along different crystallographic directions due to its preferential adsorption on specific facets, and thus cause geometrical anisotropy.^{19,20} At the beginning, Au nuclei are formed on the Au-coated Si substrate through the reduction of HAuCl_4 (step 1 in Figure 4), followed by their growth into nanostructures with tips (step 2 in Figure 4). During the electrodeposition process, PVP plays an important role due to its preferential adsorption on specific facets. On the basis of our results and the previous reports,^{3,4} we believe that PVP preferentially adsorbs on the {111} planes of Au nuclei and consequently the growth rate along the $\langle 111 \rangle$ direction is reduced while the growth rate along the $\langle 100 \rangle$ direction is enhanced, facilitating the formation of Au nanotowers. For one crystal nucleus on Si substrate, there are four {111} planes with different orientations, which can develop into tower-shaped structure with {111} facets serving as the tower's faces (step 3 in Figure 4). This stage is dominated by oriented attachment mechanism, involving attachment, rotation and realignment,^{21,22} being similar to the formation of Co dendritic nanostructures.²³ Also, Ostwald ripening plays an important role in the formation of smooth surface and regular shape of the final polycrystals (step 4 in Figure 4). In addition, there inevitably exist some outshoots on the growing tower's surfaces. Such outshoots will grow and lead to the formation of secondary hierarchy towers with {111} facet serving as the secondary tower's faces due to the same reason (step 5 in Figure 4). Similarly, third or even fourth hierarchy towers could be formed on the as-grown towers so that Au hierarchical micro/nanotowers are formed in the end (see step 5 in Figure 4).

In order to obtain highly enhanced Raman signals, Ag nanoparticles were further electrodeposited onto the surfaces of the Au hierarchical micro/nanotowers (Figure 5a,b) as Ag nanoparticles can improve the surface roughness of the micro/nanotowers and Ag exhibits the most effective SERS effect among all metals in the visible region.^{24–28} To optimize Ag-nanoparticle-decorated Au hierarchical micro/nanotowers for the best SERS effect, Ag electrodeposition with different

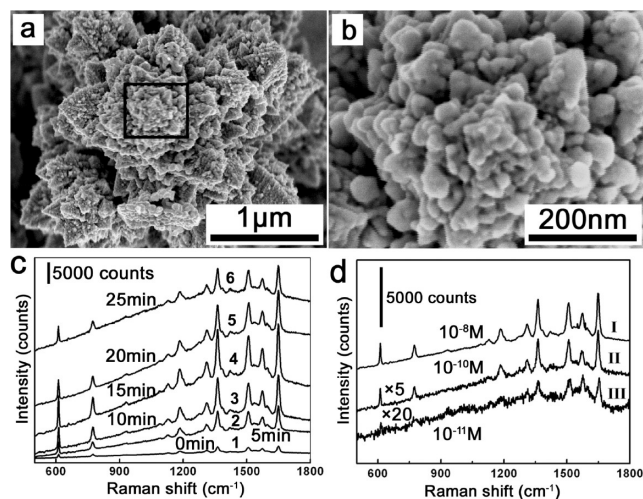


Figure 5. SEM images of the Ag-nanoparticle-decorated Au hierarchical micro/nanotower at (a) low and (b) high magnifications, respectively. Panel (b) is taken from the marked area in (a). (c) SERS spectra of 10^{-6} M R6G adsorbed on the Ag-nanoparticle-decorated Au hierarchical micro/nanotowers achieved by different Ag deposition durations. (d) SERS spectra taken from the Ag-nanoparticle-decorated Au micro/nanotowers shown in (a) after being immersed in 10^{-8} M (upper curve), 10^{-10} M (middle curve), and 10^{-11} M (lower curve) R6G for 2 h, respectively. The spectra of 10^{-10} M and 10^{-11} M R6G are magnified 5 and 20 times for clarity, respectively. All the spectra were acquired at excitation 514.5 nm, and the acquisition time was 5 s.

durations were carried out for identical Au hierarchical micro/nanotowers (SEM images shown in Figure 5b and Figure S5 in the Supporting Information). Elemental mappings indicate that Ag nanoparticles were distributed uniformly on the Au micro/nanotowers (Figure S6 in the Supporting Information). Decorating Ag nanoparticles on the as-electrodeposited bare Au micro/nanotowers created a lot of Ag nanoparticles on the surfaces of the Au hierarchical micro/nanotowers (Figures 5b). Figures S5 and S6 in the Supporting Information clearly reveal that the longer the Ag electrodeposition duration is, the more the number density and the bigger the size of the decorated Ag particles are. The UV-vis spectrum of the bare Au micro/nanotowers shows a red-shifted plasmon absorption band peak at 624 nm compared with that (520–550 nm) of the Au nanospheres,³ while the UV-vis spectrum of the Ag-decorated Au micro/nanotowers reveals a blue-shifted plasmon absorption band peak at 487 compared with that of the bare micro/nanotowers (Supporting Information Part II, Figure S7).

As the Ag-nanoparticle-decorated Au hierarchical micro/nanotowers have abundant particle junctions and nanosized sharp tips that may concentrate electromagnetic field at the tip apex, evident SERS effect can be expected.¹⁴ To study their SERS effect, we used Rhodamine 6G (R6G) as probe molecules. First, R6G aqueous solution was prepared with concentration of 10^{-6} M. To ensure R6G adsorption, the substrates were immersed in R6G aqueous solutions for 2 h, taken out and rinsed thoroughly with DI water, and then dried in high-purity Ar before Raman spectral examination. SERS spectra of 10^{-6} M R6G adsorbed on the Ag-nanoparticle-decorated Au hierarchical micro/nanotowers with different Ag electrodeposition durations are displayed in Figure 5c. The bare Au hierarchical micro/nanotower arrays showed distinct SERS effect (curve 1 in Figure 5c). The characteristic bands are distinctly observed in the spectrum, such as 1362, 1509, and 1650 cm^{-1} . More importantly, the SERS signals from the

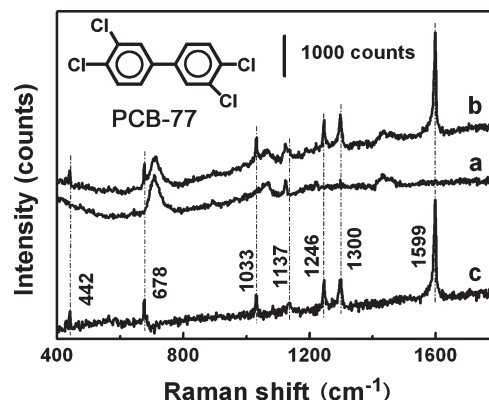


Figure 6. SERS spectra of decanethiol-modified Ag-nanoparticle-decorated Au hierarchical micro/nanotower arrays (a) before, and (b) after 10^{-3} M PCB-77 exposure for 4 h, and (c) the difference spectrum of (a) subtracted from (b). The acquisition time was 60 s.

Ag-nanoparticle-decorated Au hierarchical micro/nanotower arrays (curves 2–6 in Figure 5c) are indeed enhanced much more than that of the bare Au hierarchical micro/nanotower arrays (curve 1 in Figure 5c), indicating that the SERS effect was significantly improved via surface decorating Ag nanoparticles due to both the Ag hot spots themselves and the hot spots formed at the interfaces between Ag nanoparticles and Au nanotowers.^{17,18} As expected, the peak intensities increase with the Ag electrodeposition duration in the first 15 min, then decrease as more Ag nanoparticles grow on the surface of the Au hierarchical micro/nanotowers. With further elongation of the Ag electrodeposition duration, the Ag nanoparticles tend to connect together (Figure S6f in the Supporting Information) and the surface roughness of the micro/nanotowers will be reduced, therefore the peak intensities decrease accordingly.

To explore their ability to detect lower concentration R6G, the R6G aqueous solutions with concentrations of 10^{-8} , 10^{-10} , and 10^{-11} M were confected, and the optimal Ag-nanoparticle-decorated Au hierarchical micro/nanotowers were used as SERS substrate. The SERS spectra of R6G (Figure 5d) from different R6G concentrations adsorbed on the optimal Ag-nanoparticle-decorated Au hierarchical micro/nanotowers reveal that a low R6G concentration of 10^{-11} M (curve III in Figure 5d) can be detected.

For practical application, the SERS substrates are required to have good reproducibility. The SERS signals from seven points randomly chosen on the Ag-nanoparticle-decorated Au hierarchical micro/nanotower arrays are very similar (Figure S8 in the Supporting Information). Most other points investigated under the same experimental conditions can give quite similar SERS signals of R6G molecules; therefore, the Ag-nanoparticle-decorated Au hierarchical micro/nanotower arrays have indeed shown good reproducibility for the SERS measurements.

Then it is further demonstrated that the Ag-nanoparticle-decorated Au hierarchical micro/nanotower arrays also can be used as effective SERS substrate for rapid detection of polychlorinated biphenyls (PCBs), which belong to one kind of persistent organic pollutants (POPs) as defined in the Stockholm Convention.²⁹ PCBs are capable of bioaccumulating in humans and other animals, biomagnifying in the food chain, and imposing a big threat to the environment and humans.^{30,31} Because PCBs cannot be easily adsorbed onto the surface of Ag nanoparticles and Au micro/nanotowers, a

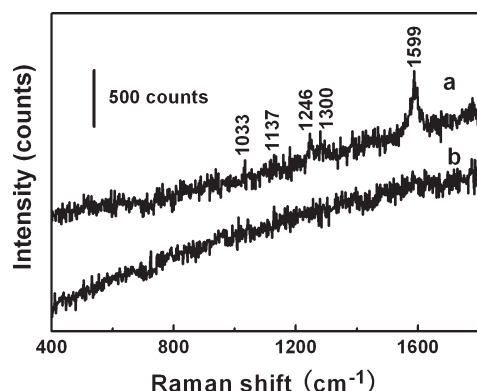


Figure 7. SERS spectra taken from the optimal Ag-nanoparticle-decorated Au hierarchical micro/nanotower arrays after (curve a) 10^{-6} and (curve b) 10^{-7} M PCB-77 exposure, respectively. The acquisition time was 60 s.

partition layer (decanethiol self-assembled layer) was assembled onto the SERS substrate to concentrate the target PCB molecules within the surfaces of the SERS substrate through its efficient van der Waals interactions with the hydrophobic PCBs.³² Figure 6 shows the SERS spectrum of PCB-77 on the decanethiol-modified Ag-nanoparticle-decorated Au hierarchical micro/nanotower arrays. We observed the following bands belonging to PCB-77: 442 cm^{-1} (ring deformation),^{32,33} 678 cm^{-1} (C–Cl stretching),^{32,33} 1033 cm^{-1} (ring breathing),¹³ 1137 cm^{-1} (ring breathing),^{13,33} 1246 cm^{-1} (C–H wagging),³³ 1300 cm^{-1} (biphenyl C–C bridge stretching)^{32,33} and 1599 cm^{-1} (ring stretching)¹³ as shown in Figure 6 (curve c), which correspond well with the normal Raman spectrum of PCB-77 that we reported previously.³⁴ When the PCB-77 concentration was decreased to 10^{-6} M, the 1137, 1246, and 1599 cm^{-1} bands (Figure 7, curve a) could still be identified, though their intensities decreased significantly. This detection limit of PCB-77 can be further improved if better attachment of PCB-77 to the SERS substrate can be achieved. These Ag-nanoparticle-decorated Au hierarchical micro/nanotower arrays therefore show the potential to be applied as sensitive and robust SERS substrates in the environmental monitoring of some special organic pollutants.

Conclusions

In summary, Au hierarchical micro/nanotower arrays have been achieved via an electrodeposition route. The resultant Au towers have four symmetrical surfaces. Oriented attachment and Ostwald ripening play important roles in the formation of the Au hierarchical micro/nanotower arrays. The resultant Au hierarchical micro/nanotowers grow tightly on the planar Au-coated-silicon substrate, and can be used as effective SERS substrate. Via further decorating Ag nanoparticles onto the surfaces of the Au hierarchical micro/nanotowers, their SERS effect has been significantly improved. These Au–Ag metal-hybrid and geometry-hierarchical micro/nanotower arrays have shown potential application in trace detection of PCBs in the environment.

Acknowledgment. This work was financially supported by the National Basic Research Program of China (Grant 2007CB936601) and the National Natural Science Foundation of China (Grant 50972145, 10975152).

Supporting Information Available: The effect of electrodeposition conditions on the morphologies of Au products; the SEM images of products achieved under different conditions; SEM images and elemental mappings of Ag-nanoparticle-decorated Au hierarchical micro/nanotowers achieved via Ag electrodeposition with different durations; the UV–vis spectra of Au hierarchical micro/nanotower arrays with and without Ag nanoparticle decoration; the SERS spectra of R6G taken from different locations on the Ag-nanoparticle-decorated Au hierarchical micro/nanotower arrays. This material is available free of charge via the Internet at <http://pubs.acs.org>.

References

- (1) Moskovits, M. *Top. Appl. Phys.* **2006**, *103*, 1.
- (2) Zhang, J. G.; Gao, Y.; Alvarez-Puebla, R. A.; Buriak, J. M.; Fenniri, H. *Adv. Mater.* **2006**, *18*, 3233.
- (3) Xu, J.; Li, S. Y.; Weng, J.; Wang, X. F.; Zhou, Z. M.; Yang, K.; Liu, M.; Chen, X.; Cui, Q.; Cao, M. Y.; Zhang, Q. Q. *Adv. Funct. Mater.* **2008**, *18*, 277.
- (4) Duan, G. T.; Cai, W. P.; Luo, Y. Y.; Li, Z. G.; Li, Y. *Appl. Phys. Lett.* **2006**, *89*, 211905.
- (5) Gao, S. Y.; Zhang, H. J.; Wang, X. M.; Yang, J. H.; Zhou, L.; Peng, C. Y.; Sun, D. H.; Li, M. Y. *Nanotechnology* **2005**, *16*, 2530.
- (6) Li, K.; Clime, L.; Cui, B.; Veres, T. *Nanotechnology* **2008**, *19*, 145305.
- (7) Lee, S. J.; Morrill, A. R.; Moskovits, M. *J. Am. Chem. Soc.* **2006**, *128*, 2200.
- (8) Zhou, Q.; Li, Z. C.; Yang, Y.; Zhang, Z. J. *J. Phys. D: Appl. Phys.* **2008**, *41*, 152007.
- (9) Sun, Y. G.; Wiederrecht, G. P. *Small* **2007**, *3*, 1964.
- (10) Liu, G. Q.; Cai, W. P.; Kong, L. C.; Duan, G. T.; Lü, F. J. *J. Mater. Chem.* **2010**, *20*, 767.
- (11) Hou, Y. M.; Xu, J.; Wang, P. W.; Yu, D. P. *Appl. Phys. Lett.* **2010**, *96*, 203107.
- (12) Liang, H. Y.; Li, Z. P.; Wang, W. Z.; Wu, Y. S.; Xu, H. X. *Adv. Mater.* **2009**, *21*, 4614.
- (13) Gütés, A.; Carraro, C.; Maboudian, R. *J. Am. Chem. Soc.* **2010**, *132*, 1476.
- (14) Sun, C. H.; Linn, N. C.; Jiang, P. *Chem. Mater.* **2007**, *19*, 4551.
- (15) Zamuner, M.; Talaga, D.; Deiss, F.; Guieu, V.; Kuhn, A.; Ugo, P.; Sojic, N. *Adv. Funct. Mater.* **2009**, *19*, 3129.
- (16) Braun, G.; Pavel, I.; Morrill, A. R.; Seferos, D. S.; Bazan, G. C.; Reich, N. O.; Moskovits, M. *J. Am. Chem. Soc.* **2007**, *129*, 7760.
- (17) Gao, L.; Fan, L. Z.; Zhang, J. *Langmuir* **2009**, *25*, 11844.
- (18) Huang, Z. L.; Meng, G. W.; Huang, Q.; Yang, Y. J.; Zhu, C. H.; Tang, C. L. *Adv. Mater.* **2010**, *22*, 4136.
- (19) Li, C. C.; Shuford, K. L.; Park, Q. H.; Cai, W. P.; Li, Y.; Lee, E. J.; Cho, S. O. *Angew. Chem., Int. Ed.* **2007**, *46*, 3264.
- (20) Kim, F.; Connor, S.; Song, H.; Kuykendall, T.; Yang, P. D. *Angew. Chem., Int. Ed.* **2004**, *43*, 3673.
- (21) Penn, R. L.; Banfield, J. F. *Science* **1998**, *281*, 969.
- (22) Penn, R. L.; Banfield, J. F. *Geochim. Cosmochim. Acta* **1999**, *63*, 1549.
- (23) Zhu, L. P.; Xiao, H. W.; Zhang, W. D.; Yang, Y.; Fu, Y. *Cryst. Growth Des.* **2008**, *8*, 1113.
- (24) Moskovits, M. *J. Raman Spectrosc.* **2005**, *36*, 485.
- (25) Tian, Z. Q.; Ren, B.; Wu, D. Y. *J. Phys. Chem. B* **2002**, *106*, 9463.
- (26) Li, W. Y.; Camargo, P. H. C.; Lu, X. M.; Xia, Y. N. *Nano Lett.* **2009**, *9*, 485.
- (27) Graham, D.; Thompson, D. G.; Smith, W. E.; Faulds, K. *Nat. Nanotechnol.* **2008**, *3*, 548.
- (28) Stokes, R. J.; Macaskill, A.; Lundahl, P. J.; Smith, W. E.; Faulds, K.; Graham, D. *Small* **2007**, *3*, 1593.
- (29) UNEP 2007 Annual Report, **2008**, p 90.
- (30) Borga, K.; Fisk, A. T.; Hargrave, B.; Hoekstra, P. F.; Swackhamer, D.; Muir, D. C. G. *Environ. Sci. Technol.* **2005**, *39*, 4523.
- (31) Borga, K.; Gabrielsen, G. W.; Skaare, J. U. *Environ. Pollut.* **2001**, *113*, 187.
- (32) Bantz, K. C.; Haynes, C. L. *Vib. Spectrosc.* **2009**, *50*, 29.
- (33) Socrates, G. *Infrared and Raman Characteristic Group Frequencies: Tables and Charts*, 3rd ed.; Wiley: New York, 2001; pp158–167.
- (34) Zhu, C. H.; Meng, G. W.; Huang, Q.; Zhang, Z.; Xu, Q. L.; Liu, G. Q.; Huang, Z. L.; Chu, Z. Q. *Chem. Commun.* **2011**, DOI: 10.1039/c0cc04482B.